

Azimuthal correlations in
photoproduction and deep inelastic
ep scattering at HERA

Additional material

ZEUS Collaboration

1 PYTHIA 8 settings

The ZEUS photoproduction data is compared to Monte Carlo events generated using PYTHIA 8.303 in the article. The main parameter of interest in this analysis is p_{T0}^{ref} , which controls the amount of Multiparton Interactions (MPI). The PYTHIA settings used are shown in Tab. 1.

| Setting type | choice(s) |
|--------------------------------|------------------------------------------|
| Beams:frameType | 2 (CM) |
| Beams:eA | 920 GeV |
| Beams:eB | 27.52 GeV |
| Beams:idA | 2212 |
| Beams:idB | 11 |
| PDF:lepton2gamma | on (enables photon sub-beam from lepton) |
| Photon:Q2max | 1.0 GeV ² |
| Photon:Wmin | 10 GeV |
| Photon:ProcessType | 0 (auto mix of resolved and direct) |
| PhotonParton:all | on or off (direct component) |
| SoftQCD:nonDiffractive | on or off (resolved component) |
| PartonLevel:MPI | on or off (master switch for MPI) |
| MultipartonInteractions:pT0Ref | 2, 3, 4 GeV (MPI strength) |
| ColourReconnection:range | 0.0, 1.8 (range in p-space of CR) |

Table 1: PYTHIA 8.303 settings used to generate PhP MC data.

Generated charged particles are retained if they satisfy the definition of primary listed in the article. About 10 M events with $N_{\text{ch}} \geq 20$ are generated for each variation.

2 Supplementary figures

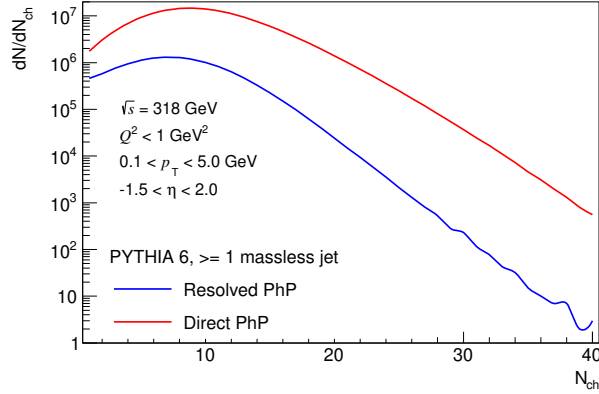


Figure 1: Generator-level distributions of charged particles for the resolved and direct photoproduction components of ZEUS light-flavor jet PYTHIA 6 PhP Monte Carlo.

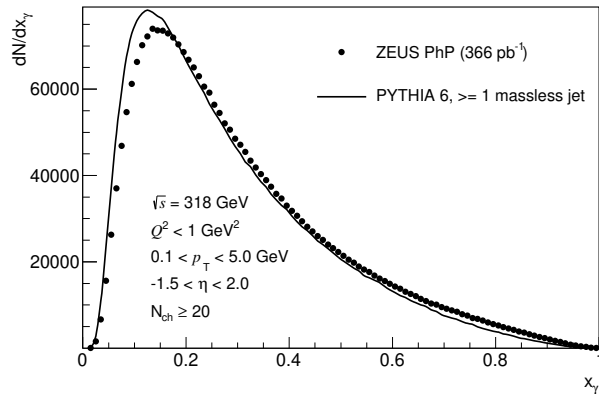


Figure 2: Reconstructed x_γ distribution in ZEUS PhP data compared to ZEUS light-flavor jet PYTHIA 6 PhP Monte Carlo. x_γ was reconstructed using the two leading jets and represents the fraction of the exchanged-photon energy and longitudinal momentum that is given to the observed particle production. Massive jets were reconstructed with E-scheme and in inclusive mode. Dead material corrections are applied. Jets are required to have transverse energy greater than 2.5 GeV and pseudorapidity in range from -2.5 to 2.5.

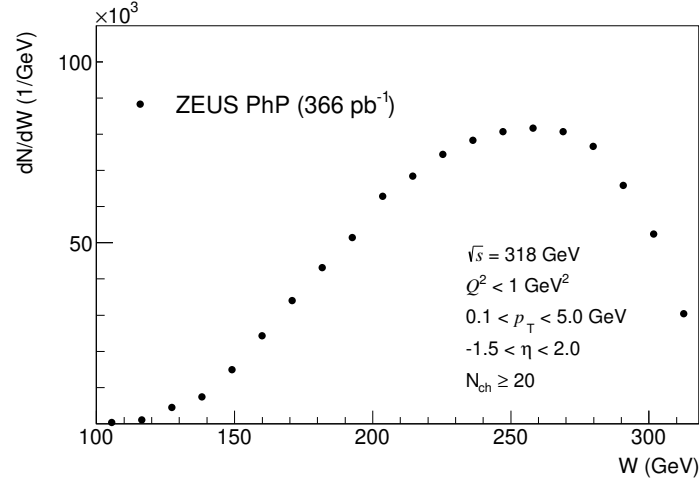


Figure 3: Reconstructed W distribution in ZEUS PhP data compared. $W = \sqrt{2 E_p (E - p_Z)}$, which corresponds to the γp centre-of-mass energy. $E - p_Z$ was measured using ZEUS final-state energy-flow objects. The mean and RMS of the ZEUS distribution is 239 and 43 GeV, respectively.

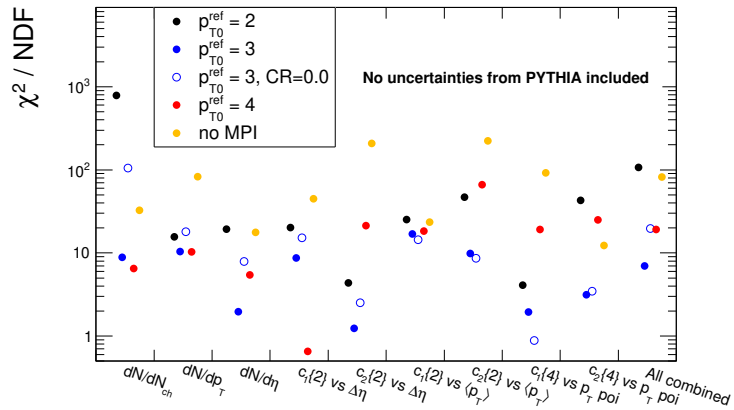


Figure 4: Compressed overview of the comparison between ZEUS PhP data and PYTHIA 8 predictions. χ^2 is computed using the combined statistical and systematic uncertainties of ZEUS data. No uncertainties from PYTHIA predictions were included. The type of observable is shown on the x-axis.

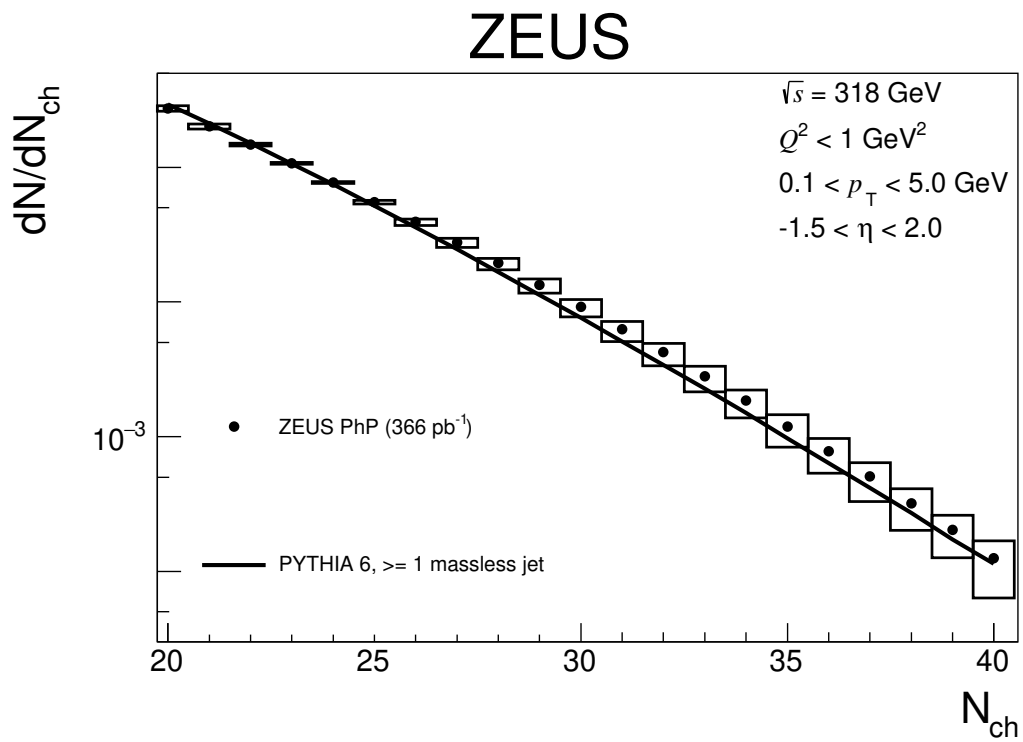


Figure 5: Charged particle multiplicity distribution dN/dN_{ch} compared to ZEUS light-flavor jet PYTHIA 6 PhP Monte Carlo. The integral of the distributions in the range shown are normalised to unity. The statistical uncertainties are shown as vertical lines although they are typically smaller than the marker size. Systematic uncertainties are shown as boxes.

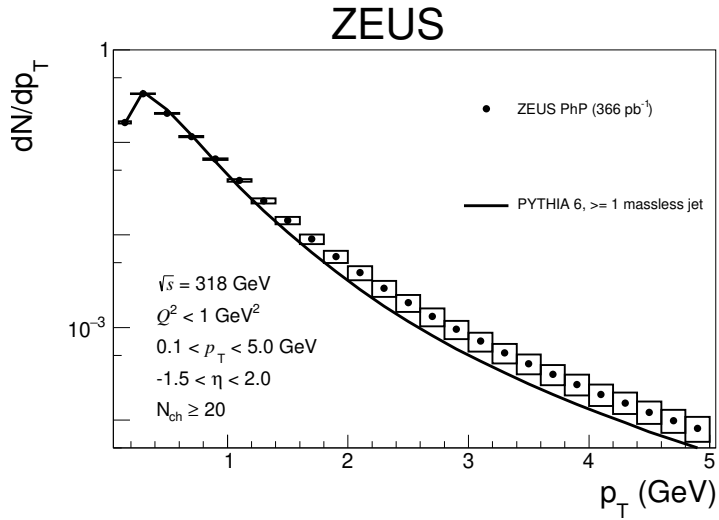


Figure 6: Charged particle transverse momentum distribution dN/dp_T . The other details (except for normalisation) are as in figure 5.

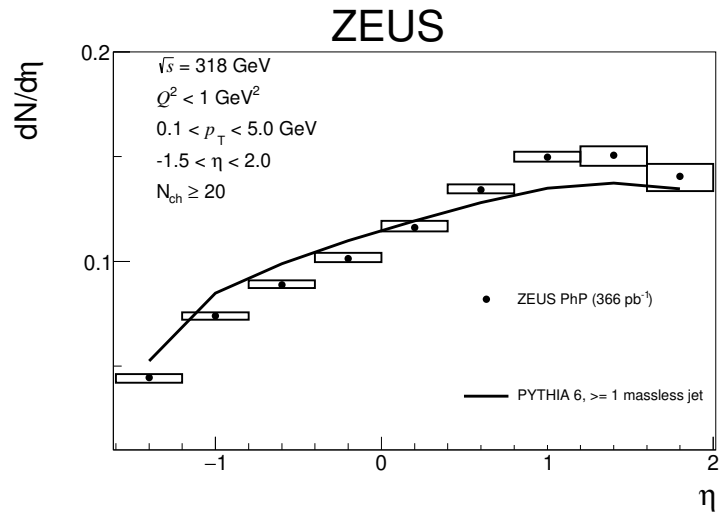


Figure 7: Charged particle pseudorapidity distribution $dN/d\eta$. The other details (except for normalisation) are as in figure 5.

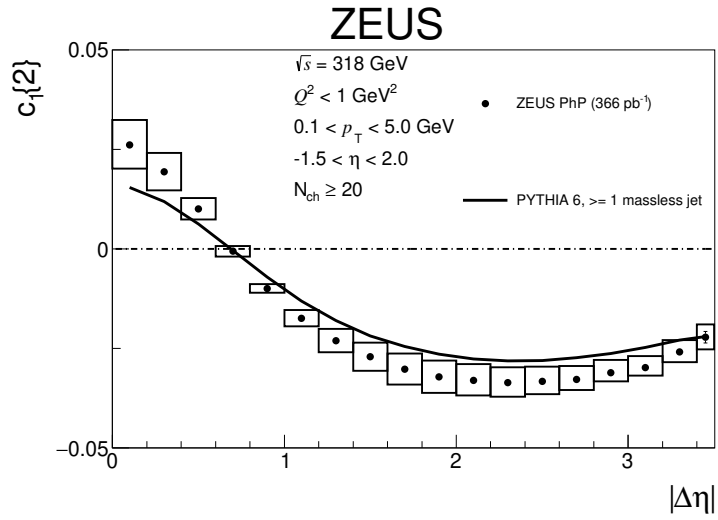


Figure 8: Two-particle azimuthal correlations $c_1\{2\}$ versus $|\Delta\eta|$. The other details (except for normalisation) are as in figure 5.

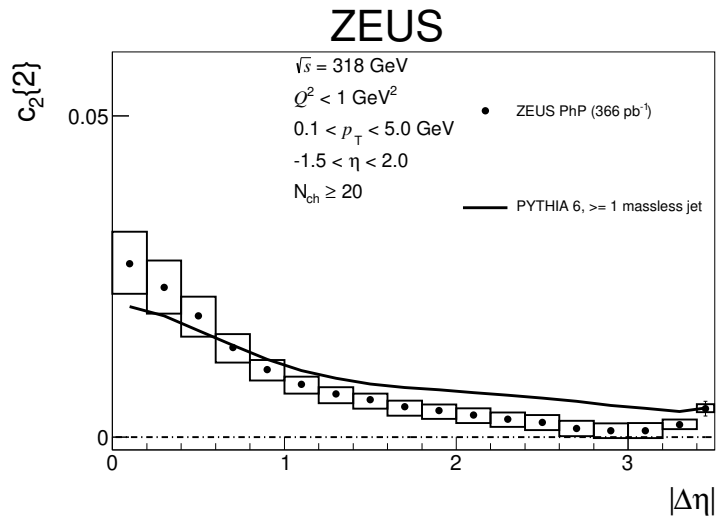


Figure 9: Two-particle azimuthal correlations $c_2\{2\}$ versus $|\Delta\eta|$. The other details (except for normalisation) are as in figure 5.

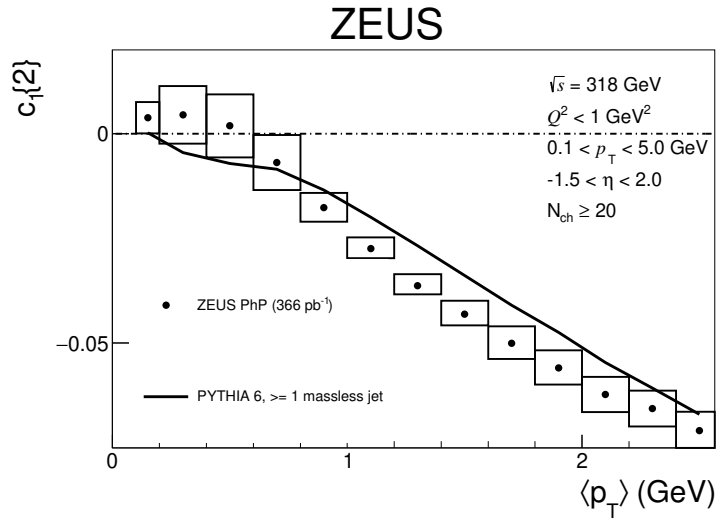


Figure 10: Two-particle azimuthal correlations $c_1\{2\}$ versus $\langle p_T \rangle$. The other details (except for normalisation) are as in figure 5.

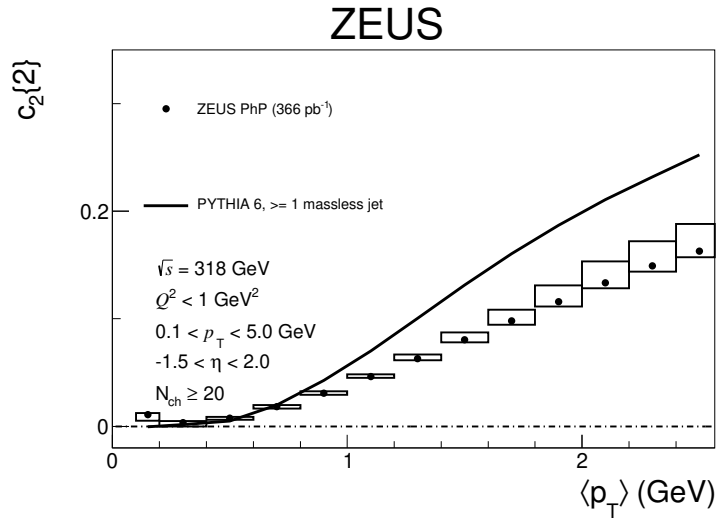


Figure 11: Two-particle azimuthal correlations $c_2\{2\}$ versus $\langle p_T \rangle$. The other details (except for normalisation) are as in figure 5.

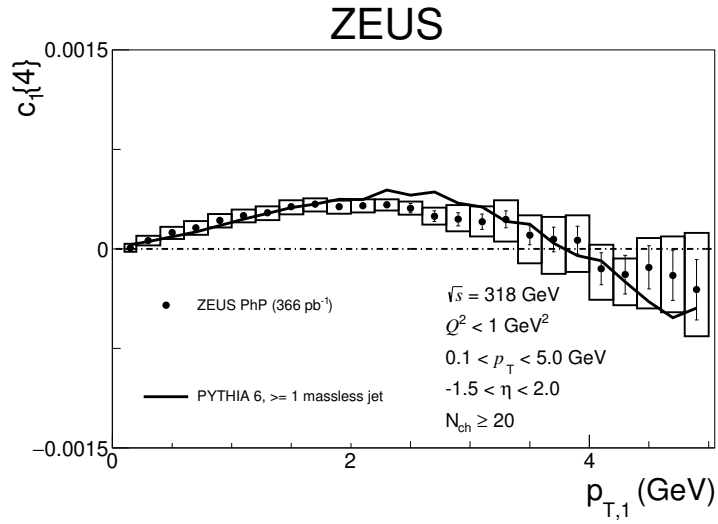


Figure 12: Four-particle azimuthal correlations $c_1\{4\}$ versus $p_{T,1}$. The other details (except for normalisation) are as in figure 5.

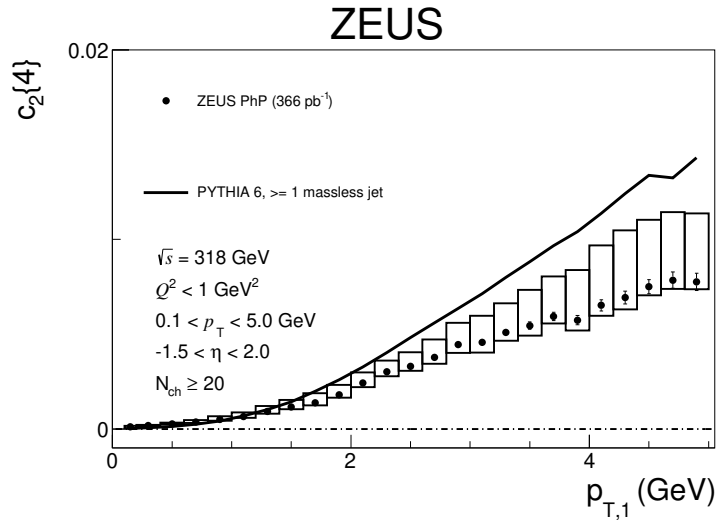


Figure 13: Four-particle azimuthal correlations $c_2\{4\}$ versus $p_{T,1}$. The other details (except for normalisation) are as in figure 5.